Gold Nanoparticle Capped Citrate as a Ligand for Chromium(III) Ion: Optimization and Its Application in Contaminated Tap Water

Eman Turky Shamkhy[1*] and Amjed Mirza Oda[2]

[1]*Department of Basic Science, College of Dentistry, University of Baghdad, Iraq*

[2]*Department of Chemistry, College of Sciences, University of Babylon, Babylon 51002, Iraq*

** **Corresponding author:***

tel: +964-7714627857
email: Emanturky.832017@gmail.com

Received: January 30, 2022
Accepted: April 1, 2022

DOI: 10.22146/ijc.72651

Abstract: *Citrate-capped gold nanoparticle (GNP) was used as a ligand for chromium chelating, and chromium ions reaction led to GNP aggregation. The color change of GNP by aggregation in the presence of chromium is a simple and rapid colorimetric test for these ions in an aqueous solution. GNP capped citrate was prepared by the citrate method and characterized by TEM, and its particle size was 20 nm. Also, the surface plasmon resonance (SPR) peak was 520 nm. In the presence of chromium ions, the color of GNP at 520 nm was shifted to 650 nm because of aggregation to give a signal as a ratio of $A_{650/520}$ more than one and proportional with chromium concentration directly. The optimum conditions were studied to obtain the high signal represented by the volume of GNP, reaction kinetic of A_{650} with time, selectivity, and interferences of Zn(II), Fe(III), Fe(II), Sn(II), Ni(II), Ca(II), Al(III), Sr(II), Cu(II), Mn(II), Co(II), Mg(II), Ag(I), and Pb(II) ions. The calibration curve is linear in the range of 100–500 ppb, and the regression was 0.9951 and applied on tap water chromium ions in the same range in the regression of 0.95. This method was simple, rapid reaction, consumed low volumes of sample, and had low detection limits. It can be recommended as a new method for chromium (III) detection in aqueous solutions.*

Keywords: *citrate; chromium(III); nanoparticle; gold capped; tap water*

■ INTRODUCTION

The entering of heavy metal wastes as a result of increased industrial use through numerous channels generates very effective harm to the environment and humankind. Lead, copper, iron, zinc, nickel, cobalt, cadmium, chromium, mercury, gold, and silver are all heavy metals that are not biodegradable. Heavy metal uptake from the surrounding environment via the food chain results in the presence and enrichment of higher species tens of thousands of times, and human ingestion via the food chain could result in chronic poisoning. In vivo, high Cr absorptions can cause fibroproliferative disease, airway hypersensitivity, nasal cancer, lung cancer, and other cancers. Exposure to Cr can produce different point mutations in DNA, chromosomal damage, and oxidative alterations in proteins in addition to adduct formation. Because each form of Cr has a different level of toxicity, the health impacts of each are varied [1-3]. Dispersive liquid-liquid microextraction and dried-droplet laser ablation ICP-MS [4], carbon composite-PVC based membrane coated platinum electrode, amperometric enzyme-based sensor [5], flame atomic absorption spectrometry [6], fluorine-doped graphite pencil electrode [7], and nano-Au/TiO_2 photocatalysis reduction with low-cost instrumentation requirements, as well as simple operation and quick results [8], and immunochromatographic assay were rapid and simple detection of chromium ion [9].

The wide range of uses for metal nanoparticles in sensing, catalysis, electronics, and photonics has a huge interest [10]. GNPs are of special interest because of their good biocompatibility, conductivity, and high surface-to-volume ratio, which have made them useful in environmental monitoring and biological sensing [11]. GNPs are commonly employed in electroanalysis [12], biosensors [13], colorimetric detection [14], and other applications. It is straightforward and quick to use

a colorimetric detection approach based on monitoring the color change caused by GNP aggregation or corrosion. Also, heavy metal ions have been detected using this technology extensively [15-16].

In this research, simple colorimetric detection of chromium ions was demonstrated good sensing at trace concentration. The procedure was based on the GNP aggregation to give a clear signal and shift from red to blue midnight color. GNP was synthesized by the citrate method and characterized by TEM, and the detection was optimized according to the volume of GNP and aggregation dependence time. Also, the selectivity and interferences were studied, and a calibration curve of pure and tap water was established.

■ EXPERIMENTAL SECTION

Materials

Gold(III) chloride trihydrate ($HAuCl_4 \cdot 3H_2O$) and sodium citrate were sourced from Sigma-Aldrich. Salts of Cu^{2+}, Ag^{+}, Ca^{2+}, Cd^{2+}, Zn^{2+}, Mg^{2+}, Sn^{2+}, Fe^{2+}, Fe^{3+}, Al^{3+}, Sr^{2+}, and Ni^{2+} were purchased from Thompson baker, India. Acetic acid and chromium salt were supplied from GCC.

Instrumentation

Transmission electron microscopy (TEM) measurements were carried out using a Zies transmission electron microscope operating at 100 kV. A drop of the GNP solution was placed on a copper grid and air-dried before the measurement. The UV-visible absorption spectra were obtained using a PerkinElmer Lambda 25 spectrophotometer.

Procedure

Synthesis of GNP

GNP capped citrate with a diameter of 20 nm was prepared by reducing 1 mM of $HAuCl_4$ by sodium citrate (1%) according to [17-18] with slight modification. Briefly, 10 mL of $HAuCl_4$ was heated nearing boiling temperature, and 1 mL of citrate solution was added rapidly. The solution was stirred continuously, and the yellow color of gold ions was fainted to colorless. Then blue sky color is appeared and darkens into dark blue, turning to cherry red color after 15 min of heating. Mixing was continued till cooling to room temperature, and the dark red mixture was filtered with a 0.22 μM Millipore membrane filter, then GNP solution was used for detection freshly.

Optimization of chromium ions detection

Several experiments were done to optimize the final conditions for chromium detection by GNP. Firstly, the reaction of chromium ions with GNP capped citrate is limited and sensitive to acetic acid addition, where at a certain volume, the aggregation is triggered and changes the color. Therefore, acetic acid 1% (v/v) is used in the following additions (5, 10, 15, 20, 25, and 30 μL) to 300 μL of GNP, and the color change was monitored for 15 min, where no change in color is the volume that GNP is stable. The color is stable at 25 μL and enough to give a final change in color after the addition of 200 ppb chromium ions. Also, the development of color was monitored after the addition of chromium ions (200 ppb), and the absorbance at 650 was measured with time for 10 min to establish a stable signal. GNP volume was studied in the various volume of GNP (100, 200, 300, 400, 500, and 600 μL) to validate the high signal as $A_{650/520}$ in the detection of chromium ions (200 ppb). The effect of selectivity and interferences ions were Zn(II), Fe(III), Fe(II), Sn(II), Ni(II), Ca(II), Al(III), Sr(II), Cu(II), Mn(II), Co(II), Mg(II), Ag(I), and Pb(II) ions, where the volume of GNP and acetic acid were 200 μL and 25 μL, respectively, the ions were 500 ppb, and the final volume was 1 mL. All these experiments were measured at room temperature and for 10 min, and the absorbance was recorded as $A_{650/520}$.

■ RESULTS AND DISCUSSION

In Fig. 1, the UV-visible absorption spectrum of GNP is shown, where the SPR band was discovered to be located at 520 nm. The Au SPR absorption is ascribed to this band. The location of this band was consistent within 2 nm four times of GNP preparations. The shape and size of the GNP were determined using TEM techniques. The TEM picture showed three scales and described all samples with a spherical and narrow distribution of GNP. The particles were spherical or semispherical in shape and had an average size of 20 nm, as shown in Fig. 2. The cherry red of GNP is clear and has

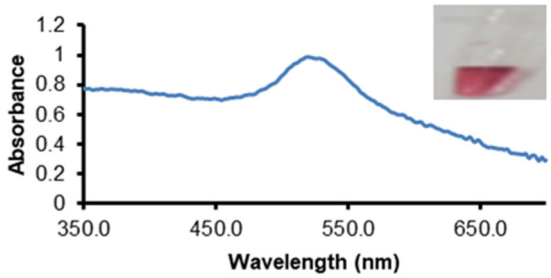

Fig 1. The absorption spectra of GNP (Inset: the red solution of prepared GNP)

good stability for 1 week, which is prepared by the citrate method many times in the same color and absorption values.

At 520 nm, GNPs with less than 60 nm have extraordinarily high extinction coefficients. Furthermore, the various aggregation phases of GNPs can cause significant color variations. These unique optical properties make GNP a suitable color-reporting candidate for signaling molecular recognition events and enable trace concentration detection. As a result, colorimetric assays based on GNP aggregation are well established as a simple and sensitive detection method. The GNPs are aggregated by an analyte of cross-linking molecules that have several binding sites for molecules immobilized on the GNP surface in the majority of these experiments [19]. This phenomenon is the base of chromium detection in aqueous solutions by GNP color change, and it is important to optimize the clear signal for a visual test. The test depends on the deep red color of GNP at the level that is visual to the naked eye, so the effect of dilution on GNP solution is studied, where the tolerance is not exceeded five times dilution. The concentration of GNP was determined and found to equal to 10.9 nM from Beer-Lambert law via UV-vis spectroscopy and based on as reported, where the extension coefficient was 8.78×10^8 M^{-1} cm^{-1} at λ_{max} 520 nm and the size was 20 nm [20]. The as-prepared GNP can be diluted to give a good signal and easily detected by the eyes. In our experiments, the dilution was 5 times applied for all experiments. In Fig. 3, the calibration curve is plotted according to the high extension coefficient as reported above, and the relationship is in a good straight line with a high correlation coefficient equal to 0.9956.

GNP stability solution is monitored for any alteration in color under storage, and we recommend it be used for not more than one weak. The storage of GNP was done in the ambient condition in our lab, and the

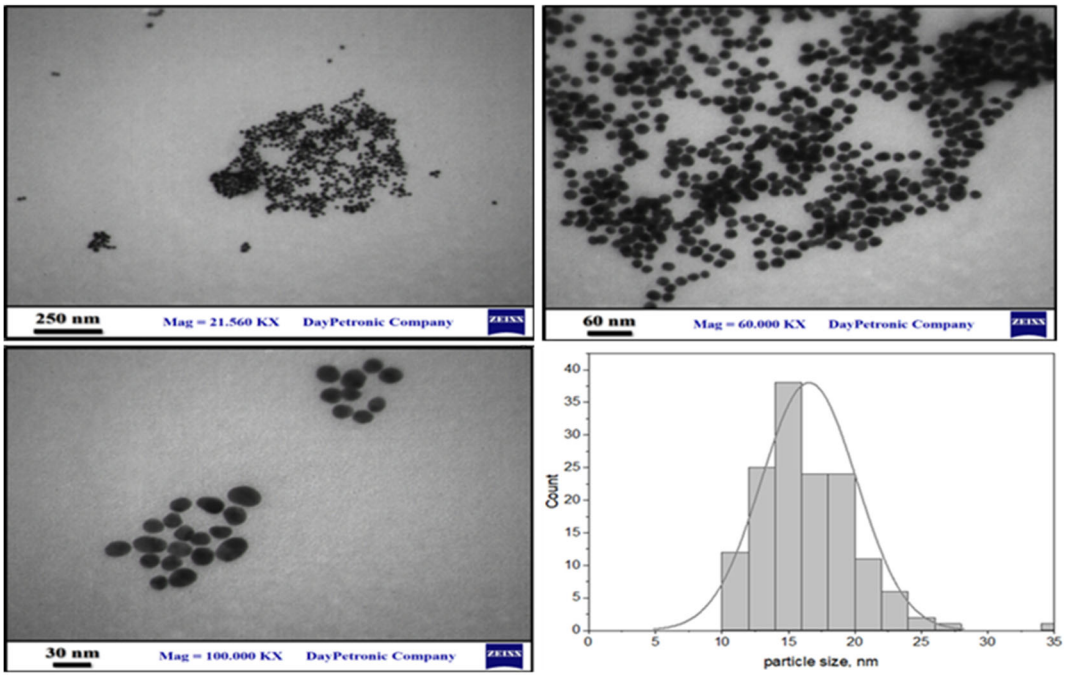

Fig 2. TEM images of GNP in different scales as prepared by citrate method and the size distribution

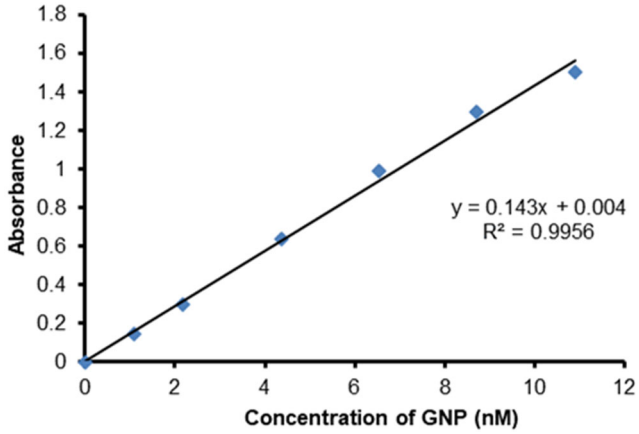

Fig 3. Correlation between GNP concentration and absorbance at 520 nm

absorbance was tested every day as absorbance at 520 nm in a UV-vis spectrophotometer. The result is not shown, but the data of absorbance was stable and changed by only 20%. This is due to self-aggregation or formation of clusters in the preparation and should be monitored with time as reported [21].

Optimization of GNP Detection

Effect of time

The color change of citrate-capped GNP is sensitive to the presence of chromium ions. This reaction depends on the aggregation of gold nanoparticles capped citrate, where the latter is the ligand probe for chromium ion masking [22]. The reaction is working on, and a fast reaction needs a second to change color from red to blue but to reach a stable blue color needing time to give a stable absorbance. The change of color is monitored by measuring the absorbance at 650 nm with time from 0–10 min to determine the optimum time and constant absorbance with time. The kinetics of aggregation was studied for A_{650} as a signal for aggregation. It was increased in steeping slope. For 3 min, the absorbance was stable, and then a plateau appeared in the range of 3–10 min. In our results, we found the rapid test by this simple procedure as the change in color is fast and indicates the presence of chromium(III) ions in aqueous solutions. The results appear in Fig. 4, which is shown the absorbance at 650 nm of gold nanoparticles solution (after aggregation) related to time in seconds. Our findings on this kinetics are agreed upon by other researchers who worked on the kinetics of gold nanoparticle aggregation [23].

Effect of GNP volume

This part aims to optimize the volume of GNP for a high detection signal in the presence of a constant concentration of chromium ions. The procedure was done by measuring the signal as A_{650}/A_{520} of the samples by adding various volumes of gold nanoparticles and chromium ions at 500 ppb. The highest signal of GNP in various volumes to detect chromium ions was 200 µL and then diluted with distilled water for a final volume of 1 mL. As the GNP volume was changed, the signal was different due to GNP capped citrate working as a ligand and aggregating around chromium ion to give the highest signal. At a low volume of GNP, the change in

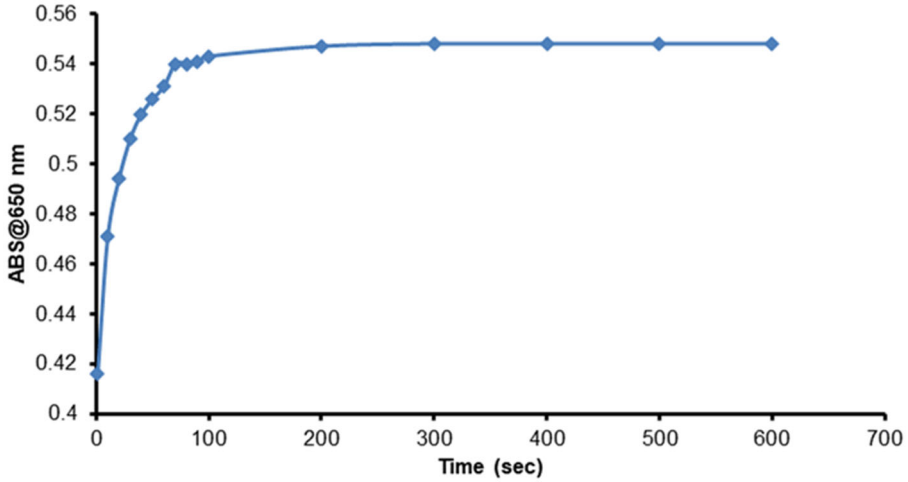

Fig 4. The kinetic plot of GNP as a function of time (200 ppb of chromium, 200 µL of GNP, and total volume is 1 mL)

color into the blue is not representing all chromium ions attaching because the ratio of reaction is low, and many chromium ions were free without reaction leading to low aggregation. Whereas at a high volume of GNP, all chromium ions are attached. But the excess of non-aggregated GNP affected the signal value, especially at A_{520}, where a high value made the final signal of absorbance ratio A_{650}/A_{520} low. We found that 200 µL of GNP as a volume is the best, where the signal was high and a low-noise red color. In Fig. 5, the volume of GNP added to chromium ions solution was effective on the signal of detection (A_{650}/A_{520}). The distinctive color was clear and gave a high signal in the form of A_{650}/A_{520}, as shown compared to other signals resulting from different GNP volumes.

Effect of acetic acid

The important factor in the color change was the addition of acetic acid (1% v/v), and we found that the trigger was this acid. In the preliminary experiment, in the absence of acetic acid, there is no change in color though chromium ion was added. Thus, this detection is very limited by acetic acid, and changing its addition was a reactive stimuli factor for detection. When the addition was less than 25 µL, there was no change in color, which gave the false-negative signal. In contrast, more than this volume, the color change into blue (aggregation by acid) despite no chromium ions being added, and this is the false-positive signal due to the salting out of GNP. Also, acetic acid could aid in the stability of GNP in an aqueous solution to keep surface charge high and zeta potential. Acetic acid gives high dispersion as the carboxylic moieties make the protection of surface [24]. There is no visual change in GNP solution at 25 µL of 1% acetic acid. It was stable for 30 min, and there was no change in absorption or wavelength. The blue color appeared in the acidified GNP solution after the addition of chromium ions, where the absorption changed and the bathochromic shift at 650 nm. The role of acetic acid as a trigger in detection is working for the acceleration of aggregation, especially when chromium ions are found [25]. In Fig. 6, the UV-vis absorption spectra red and blue line of acidified GNP solution before and after chromium ions addition, respectively, and the stacked photograph picture is the GNP before (right) and after chromium addition (left).

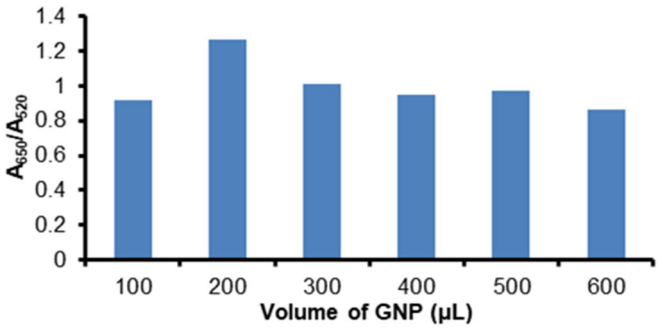

Fig 5. Effect of volume change of GNP on signal A_{650}/A_{520} in chromium detection (200 ppb)

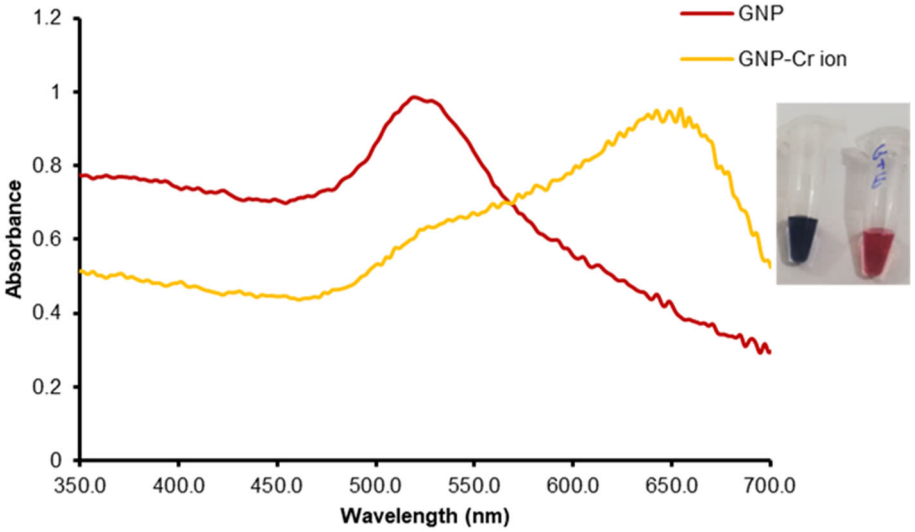

Fig 6. UV-vis spectra of GNP solution before and after detection of chromium ions

To show that citrate-capped GNP is selective for chromium ions, we studied the interaction of other ions on the signal of GNP ratio A_{650}/A_{520}. Like these ions Zn(II), Fe(III), Fe(II), Sn(II), Ni(II), Ca(II), Al(III), Sr(II), Cu(II), Mn(II), Co(II), Mg(II), Ag(I) and Pb(II) and each ions concentration was 500 ppb and chromium ions were 200 ppb. Experimentally, there is no color change of GNP with these ions compared to chromium ions. The color stays red, the signal is strong for chromium ions, and the blue color is clear visually. In Fig. 7, the representation results of selectivity of GNP toward chromium ion to give a high signal compared to other ions, and the difference is very large. All ions under study have not interacted with GNP, and their color is unchanged visually. Also, the signal of other ions is near the GNP blank with red color. This is explained that the high absorbance ratio of chromium-GNP was affected by the aggregation of GNP. In contrast, in the presence of other ions, the value of A_{650}/A_{520} was low, indicating well-dispersed forms of citrate-capped GNP. Therefore, chromium ions must selectively interact with a specific site on the surface of GNP [26].

The selectivity of this procedure is examined to detect the interference of coexisting ions. Metal ions such as ions Zn(II), Fe(III), Fe(II), Sn(II), Ni(II), Ca(II), Al(III), Sr(II), Cu(II), Mn(II), Co(II), Mg(II), Ag(I) and Pb(II) challenge this detection technique [27]. Each type of metal ion has a concentration of 500 ppb. The chromium ion concentration is chosen to be 200 ppb. All ions are added to the same solution to the GNP solution to study the interference effect of all ions on the color of GNP. The signal is almost stable for 30 min, and no color change in the absence of chromium ions. Also, the spectrum of GNP with ions is similar to the negative signal. According to the spectra in Fig. 8, the absorption at 520 nm is not changed despite the presence of interferences of ions and no difference in peak location of citrate-capped GNP and GNP with interference ions. After adding chromium ions, the absorption peak decreased at 520 nm and increased at 650 nm considerably, as reported [28]. That is an indication of interferences from all ions understudy that did not affect the signal of GNP. In Fig. 9, the $A_{650/520}$ ratio for chromium ions is greater than one. Its value exceeds the signal of A_{650}/A_{520} that belongs to GNP with or without interfered ions, where this is a very good result to estimate chromium according to this method. Also, we found the signal induction is strong in the presence of other ions as an indication that the interference ions do not affect chromium ions detection, and this method is hard resisting the interferences [29]. The signal as A_{650}/A_{520} of GNP in the presence and absence of chromium ions interfered with the ions under study is shown in Fig. 9.

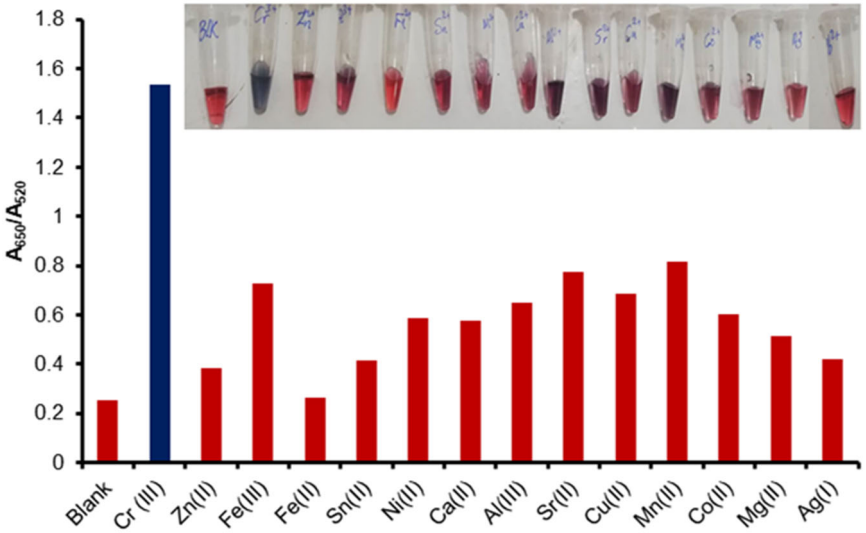

Fig 7. Ratio A_{650}/A_{520} of the chromium ions selectivity against other studied ions. Chromium ions concentration is 200 ppb, and the other ions are 500 ppb, and the stacked picture is the visual color of blank GNP (first left), chromium ions (second left), and all ions on the right

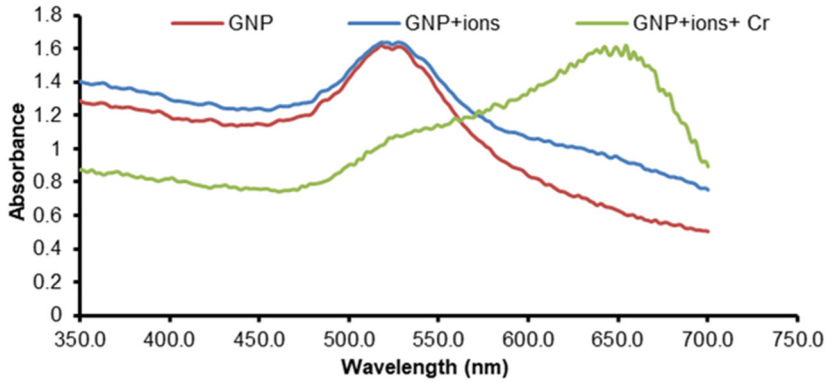

Fig 8. UV-vis spectra of GNP, GNP-interfered ions, and GNP-interfered ions after chromium ions addition. The ions are Zn(II), Fe(III), Fe(II), Sn(II), Ni(II), Ca(II), Al(III), Sr(II), Cu(II), Mn(II), Co(II), Mg(II) and Pb(II)

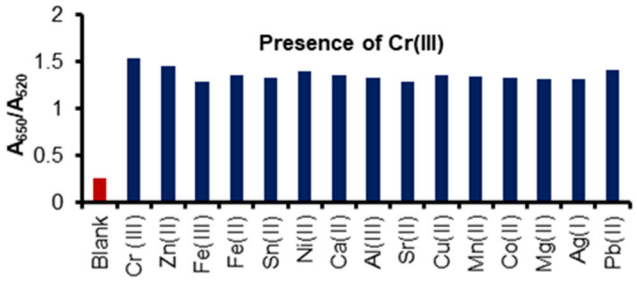

Fig 9. Signal A_{650}/A_{520} of GNP and GNP in the presence of interference ions

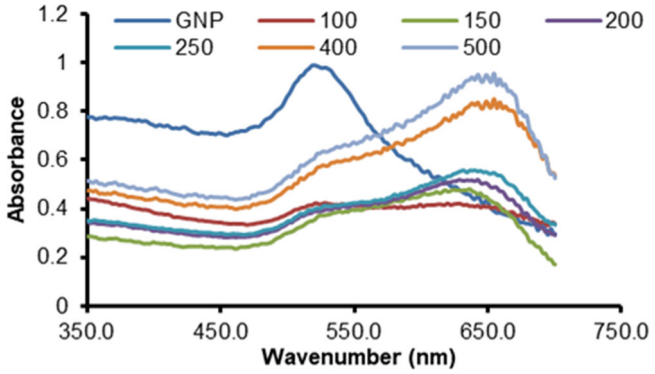

Fig 10. UV-vis spectra of GNP before and after adding standard concentrations of chromium ions

Calibration

Chromium was quantified by GNP capped citrate, where the absorption ratio of A_{650}/A_{520} was used to monitor the color change of GNP by adding various concentrations of chromium ions in the range of 100–500 ppb. We found a related signal to the changing of concentration chromium ions. As the chromium ions concentration increased, the color of the GNP solution changed from red to dark midnight blue. The understudy concentrations were 100–500 ppb, where the absorbance at 650 nm increased, whereas the peak at 520 nm decreased, as shown in Fig. 10. The absorption spectra of GNP before reaction and after reaction with chromium ions have appeared and shifted from 520 nm to 650 nm in each spectrum. The absorption ratio A_{650}/A_{520} was used as a signal, and it is different in sensitivity and proportional to chromium concentration. In this study, the calibration is ranged from 100 to 500 ppb within the linear range of the calibration curve with high regression equal to 0.9951, and the detection limit was 50 ppb was calculated according to the

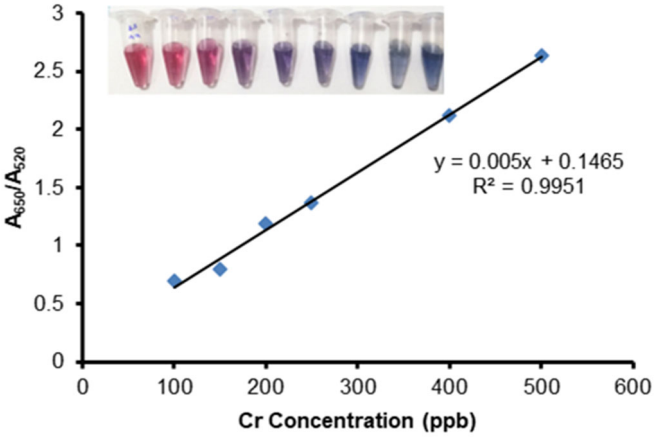

Fig 11. Calibration curve of chromium ions according to A_{650}/A_{520} of GNP, and the stacked picture is a color change of GNP

S/N = 3 rule [30]. The calibration curve of chromium ion concentration change was proportional to the signal A_{650}/A_{520}, which is illustrated in Fig. 11.

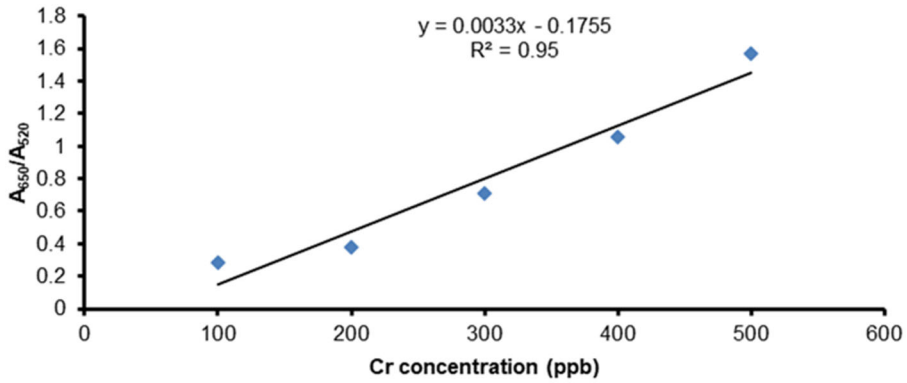

Fig 12. The application of chromium ions detection by GNP as a calibration curve

The detection application is applied on real tap water to specify the accuracy in color change and compare it with experimental calibration. The concentration of chromium ions in the range of 100–500 ppb was prepared as a sample in tap water, and GNP color change was recorded as A_{650}/A_{520}. The range of detection for chromium ions in tap water with good regression (0.95) and good signal to detect in tap water is shown in Fig. 12.

■ CONCLUSION

GNP capped citrate was prepared at particle size about 20 nm by citrate method and stable for one week and can be prepared three repeats without SPR peak change. This method is simple and rapid for chromium ions detection using GNP as a ligand. The change in color absorption decreased at 520 nm and increased at 650 nm, where the signal was more reasonable as A_{650}/A_{520}. The aggregation is affected by acetic acid addition, which accelerates the color change, and the signal A_{650}/A_{520} was affected by the volume of GNP. The signal A_{650}/A_{520} of chromium ions was not affected in the presence of Zn(II), Fe(III), Fe(II), Sn(II), Ni(II), Ca(II), Al(III), Sr(II), Cu(II), Mn(II), Co(II), Mg(II), Ag(I) and Pb(II), to be selective and less interfere chromium ions in aqueous solution. The A_{650}/A_{520} was proportional with chromium concentration, and the range was 100–500 ppb with 50 ppb as a detection limit. Also, it was applicable in tab water in the same concentration range. This method was very beneficial for chromium(III) ion detection in the lab or polluted sample, and it can be immobilized on paper lateral force test to get a more powerful and easy test.

■ REFERENCES

[1] Li, Y.T., Becquer, T., Dai, J., Quantin, C., and Benedetti, M.F., 2009, Ion activity and distribution of heavy metals in acid mine drainage polluted subtropical soils, *Environ. Pollut.*, 157 (4), 1249–1257.

[2] Nguyen, H.D., Nguyen, T.T.L., Nguyen, K.M., Tran, T.A.T., Nguyen, A.M., and Nguyen, Q.H., 2015, Determination of ppt level chromium(VI) using the gold nano-flakes electrodeposited on platinum rotating disk electrode and modified with 4-thiopyridinium, *Am. J. Anal. Chem.*, 6 (5), 457–467.

[3] Liu, X., Xiang, J.J., Tang, Y., Zhang, X.L., Fu, Q.Q., Zou, J.H., and Lin, Y., 2012, Colloidal gold nanoparticle probe-based immunochromatographic assay for the rapid detection of chromium ions in water and serum samples, *Anal. Chim. Acta*, 745, 99–105.

[4] Villaseñor, Á., Greatti, C., Boccongelli, M., and Todolí, J.L., 2017, A dried droplet calibration approach for the analysis of solid samples through laser ablation - inductively coupled plasma mass spectrometry, *J. Anal. At. Spectrom.*, 32 (3), 587–596.

[5] Han, X., Li, C., and Yong, D., 2019, Microbial electrode sensor for heavy-metal ions, *Sens. Mater.*, 31 (12), 4103–4111.

[6] Bhatt, R., Bhatt, R., and Padmaja, P., 2018, DTPA capped gold and silver nanofluids-facile synthesis and their application as chromium sensors, *Sens. Actuators, B*, 258, 602–611.

[7] Ly, S.Y., and Kim, M.J., 2009, Diagnostic assay of

chromium (VI) in the ex vivo fluid of the urine of a smoker using a fluorine-doped handmade sensor, *J. Clin. Lab. Anal.*, 23 (2), 82–87.

[8] Peng, G., He, Q., Lu, Y., Huang, J., and Lin, J.M., 2017, Flow injection microfluidic device with on-line fluorescent derivatization for the determination of Cr(III) and Cr(VI) in water samples after solid-phase extraction, *Anal. Chim. Acta*, 955, 58–66.

[9] Paek, S.H., Lee, S.H., Cho, J.H., and Kim, Y.S., 2000, Development of rapid one-step immuno chromatographic assay, *Methods*, 22 (1), 53–60.

[10] Hussein, M.A., Ganash, A.A., and Alqarni, S.A., 2019, Electrochemical sensor-based gold nanoparticle/poly(aniline-co-o-toluidine)/graphene oxide nanocomposite modified electrode for hexavalent chromium detection: a real test sample, *Polym.-Plast. Technol. Mater.*, 58 (13), 1423–1436.

[11] He, M.Q., Yu, Y.L., and Wang, J.H., 2020, Biomolecule-tailored assembly and morphology of gold nanoparticles for LSPR applications, *Nano Today*, 35, 101005.

[12] Bagheri, N., Mazzaracchio, V., Cinti, S., Colozza, N., Di Natale, C., Netti, P.A., Saraji, M., Moscone, D., and Arduini, F., 2021, Electroanalytical sensor based on gold-nanoparticle-decorated paper for sensitive detection of copper ions in sweat and serum, *Anal. Chem.*, 93 (12), 5225–5233.

[13] Liu, M., Yu, X., Chen, Z., Yang, T., Yang, D., Liu, Q., Du, K., Li, B., Wang, Z., Li, S., Deng, Y., and He, N., 2017, Aptamer selection and applications for breast cancer diagnostics and therapy, *J. Nanobiotechnol.*, 15 (1), 81.

[14] Bothra, S., Kumar, R., and Sahoo, S.K., 2015, Pyridoxal derivative functionalized gold nanoparticles for colorimetric determination of zinc(II) and aluminium(III), *RSC Adv.*, 5 (118), 97690–97695.

[15] Priyadarshini, E., and Pradhan, N., 2017, Metal-induced aggregation of valine capped gold nanoparticles: An efficient and rapid approach for colorimetric detection of Pb^{2+} ions, *Sci. Rep.*, 7 (1), 9278.

[16] Wang, Y., Wang, L., Su, Z., Xue, J., Dong, J., Zhang, C., Hua, X., Wang, M., and Liu, F., 2017, Multipath colourimetric assay for copper(II) ions utilizing MarR functionalized gold nanoparticles, *Sci. Rep.*, 7 (1), 41557.

[17] Leng, W., Pati, P., and Vikesland, P.J., 2015, Room temperature seed mediated growth of gold nanoparticles: Mechanistic investigations and life cycle assessment, *Environ. Sci.: Nano*, 2 (5), 440–453.

[18] Herizchi, R., Abbasi, E., Milani, M., and Akbarzadeh, A., 2016, Current methods for synthesis of gold nanoparticles, *Artif. Cells Nanomed. Biotechnol.*, 44 (2), 596–602.

[19] Bansal, S.A., Kumar, V., Karimi, J., Singh, A.P., and Kumar, S., 2020, Role of gold nanoparticles in advanced biomedical applications, *Nanoscale Adv.*, 2 (9), 3764–3787.

[20] Kim, D.K., Hwang, Y.J., Yoon, C., Yoon, H.O., Chang, K.S., Lee, G., Lee, S., and Yi, G.R., 2015, Experimental approach to the fundamental limit of the extinction coefficients of ultra-smooth and highly spherical gold nanoparticles, *Phys. Chem. Chem. Phys.*, 17 (32), 20786–20794.

[21] Epanchintseva, A.V., Poletaeva, J.E., Pyshnyi, D.V., Ryabchikova, E.I., and Pyshnaya, I.A., 2019, Long-term stability and scale-up of noncovalently bound gold nanoparticle-siRNA suspensions, *Beilstein J. Nanotechnol.*, 10, 2568–2578.

[22] Chang, C.C., Chen, C.P., Wu, T.H., Yang, C.H., Lin, C.W., and Chen, C.Y., 2019, Gold nanoparticle-based colorimetric strategies for chemical and biological sensing applications, *Nanomaterials*, 9 (6), 861.

[23] Zhang, Z., Ye, X., Liu, Q., Liu, Y., and Liu, R., 2020, Colorimetric detection of Cr^{3+} based on gold nanoparticles functionalized with 4-mercapto benzoic acid, *J. Anal. Sci. Technol.*, 11 (1), 10.

[24] Ejeta, S.Y., and Imae, T., 2021, Selective colorimetric and electrochemical detections of Cr(III) pollutant in water on 3-mercaptopropionic acid-functionalized gold plasmon nanoparticles, *Anal. Chim. Acta*, 1152, 338272.

[25] Iglesias, E., 2020, Gold nanoparticles as colorimetric sensors for the detection of DNA bases and related compounds, *Molecules*, 25 (12), 2890.

[26] Kim, K.M., Nam, Y.S., Lee, Y., and Lee, K.B., 2018, A highly sensitive and selective colorimetric Hg^{2+} ion probe using gold nanoparticles functionalized with polyethyleneimine, *J. Anal. Methods Chem.*, 2018, 1206913.

[27] Salimi, F., Kiani, M., Karami, C., and Taher, M.A., 2018, Colorimetric sensor of detection of Cr(III) and Fe(II) ions in aqueous solutions using gold nanoparticles modified with methylene blue, *Optik*, 158, 813–825.

[28] Jin, W., Huang, P., Chen, Y., Wu, F., and Wan, Y., 2015, Colorimetric detection of Cr^{3+} using gold nanoparticles functionalized with 4-amino hippuric acid, *J. Nanopart. Res.*, 17 (9), 358.

[29] Jian-feng, G., Chang-jun, H., Mei, Y., Dan-qun, H., Jun-jie, L., Huan-bao, F., Hui-bo, L., and Ping, Y., 2016, Colorimetric sensing of chromium(VI) ions in aqueous solution based on the leaching of protein-stabled gold nanoparticles, *Anal. Methods*, 8 (27), 5526–5532.

[30] Karami, C., Arkan, E., and Arabi, M.S., 2019, Detection of chromium(III) in drinking water with modified gold nanoparticle, *Desalin. Water Treat.*, 165, 197–202.